Excess Electron Transfer in DNA: Effect of Base Sequence and Proton Transfer

Zhongli Cai, Xifeng Li, and Michael D. Sevilla*

Department of Chemistry, Oakland University, Rochester, Michigan 48309-4477

Received: October 18, 2001; In Final Form: December 3, 2001

The effect of base sequence on excess electron transfer (ET) along the DNA "π-way" is investigated in this work by use of various polynucleotide duplexes and salmon sperm DNA. Studies in frozen glassy aqueous solutions (7 M LiBr−D_2O) of the duplexes polydAdT·polydAdT and polydIdC·polydIdC randomly intercalated with mitoxantrone (MX) are compared with our previously reported data on electron transfer in DNA−MX systems. The values of electron tunneling constant β and ET distances at 1 min are found to be 0.75 ± 0.1 $Å^{-1}$ and 9.4 ± 0.5 bp for pdAdT·pdAdT (D_2O) and 1.4 ± 0.1 $Å^{-1}$ and 5.9 ± 0.5 bp for pdIdC·pdIdC (D_2O), vs 0.92 ± 0.1 $Å^{-1}$ and 9.5 ± 1.0 bp for DNA (D_2O) reported previously. The β value for DNA lies intermediate between that for pdAdT·pdAdT (0.75 $Å^{-1}$) and that for pdIdC·pdIdC (1.4 $Å^{-1}$). These results suggest that deuteron transfer from I to $C•^-$ forming CD• significantly slows but does not stop electron transfer. Similarly, in DNA proton transfer in GC anion radical is not found to stop electron transfer. The lower value of β for pdAdT·pdAdT is expected since proton transfer in the AT base pair is not energetically favorable. A study with DNA in glassy H_2O solutions was performed. The β found (0.83 ± 0.1 $Å^{-1}$) is close to that found in glassy D_2O solutions (0.92 ± 0.1 $Å^{-1}$) but may suggest a modest isotope effect. Electron and hole transfer processes in frozen solutions (D_2O ices) of polyA·polyU−MX and polyC·polyG−MX are also studied and compared with our previously reported data on electron and hole transfer in frozen D_2O solutions of DNA−MX. We find electron/hole transfer in polyA·polyU is significantly further than in DNA and transfer distances in polyC·polyG are substantially less than in DNA, which confirm our results in aqueous glasses.

Introduction

A number of recent experimental and theoretical studies have shed light on the hole transfer mechanisms and factors that influence hole transfer rate within DNA.[1−6] As a consequence, the development of our understanding of DNA hole transfer processes has progressed rapidly of late. However, excess electron transfer (ET) has not received the same attention and our efforts are among the few investigations in recent work that explicitly investigate excess electron transfer.[7−13] Our earlier efforts on excess electron transfer showed that single-step tunneling occurs in DNA at low temperatures. We reported an overall distance decay constant β near 0.9 $Å^{-1}$ for DNA in frozen aqueous glasses.[9] We also found electron transfer between DNA duplexes (ds) was competitive with transfer along the duplex when the DNA duplexes approached within ca. 40 Å (axis center to center distance) of each other. These results led to a three-dimensional model that accounts for the electron transfer both along DNA duplex and across to adjacent DNA duplexes.[10] Our studies on the effects of hydration, polymeric and aliphatic amine cations, and nucleosome proteins on electron and hole transfer in γ-irradiated DNA[12] supported this three-dimensional model for interduplex transfer.[7b] We also probed into the temperature effects (from 4 to 195 K) on excess electron and hole transfer through DNA and assigned the ranges of temperature where tunneling, reversible and irreversible protonations, hopping, and recombination reactions make contributions.[11] Finally, in our recent theoretical work proton transfer reactions in the GC and IC anion and cation radicals are treated by density functional theory to aid our understanding of the possible contributions of these reactions to electron and hole transfer in DNA.[14] These studies shed light on fundamental electron transfer processes in DNA and are important to the understanding of the damage to DNA from exposure to ionizing irradiation.

In the present work we investigate the effect of base sequence on excess electron transfer within DNA and consider the effects of proton transfer reactions between base pairs. Experimental works by Steenken[15] and our own theoretical works[14,16] on the thermodynamic driving force for proton transfer within the base pair both suggest that proton transfer is favorable in $GC•^-$, while it is less favorable in $GC•^+$ (theory suggests it is slightly unfavorable,[14] and arguments from experiments suggest it is slightly favorable[15]). While there are two studies on the effect of deprotonation of $G•^+$ on hole transfer in DNA duplexes,[17] there is no report that directly investigates the effect of protonation reactions on excess electron transfer through DNA. Several reports suggest that electron and hole transfer in DNA is sensitive to base sequence.[1,2,18a−c] However, most studies on this issue were performed at room temperature and could not isolate tunneling and hopping processes.

In this work we employ electron spin resonance (ESR) spectroscopy to investigate the effects of proton transfer and base sequence on electron tunneling in DNA at 77 K. Electron transfer in several polynucleotides, (1) polydAdT·polydAdT, (2) polydIdC·polydIdC, (3) polyA·polyU, and (4) polyC·polyG, randomly intercalated with mitoxantrone (MX), are followed in frozen glassy 7 M LiBr aqueous (D_2O) solutions (1, 2) or frozen aqueous solutions (3, 4). In addition, electron transfer from DNA anion radical donors to the intercalated MX acceptor is followed with time in frozen glassy 7 M LiBr aqueous (H_2O) solutions and compared with our previous results in glassy D_2O

* To whom correspondence should be addressed. Fax: 248 370 2321. E-mail: sevilla@oakland.edu.

10.1021/jp013881k CCC: $22.00
Published on Web 02/09/2002

solutions. Our techniques have the advantage that the donors, DNA base radicals, and the resultant acceptor radical, MX•, are identified and followed with time.

Experimental Section

Sample Preparation. *Dialysis.* Polydeoxyadenylic−thymidylic acid sodium salt (polydAdT·polydAdT, average length = 4219 bp), polydeoxyinosinic−deoxycytidylic acid sodium salt (polydIdC·polydIdC, reported distribution from 150 to 550 bp in length), polydeoxyguanylic−deoxycytidylic acid sodium salt (polydGdC·polydGdC, average length = 750 bp), polydeoxyguanylic−polydeoxycytidylic acid sodium salt (polydG·polydC, average length = 8560 bp), polyadenylic−polyuridylic acid sodium salt (polyA·polyU, reported distribution from 100 to 2000 bp), and polycytidylic−polyguanylic acid sodium salt (polyC·polyG) were from Sigma. Due to the contamination of nitrate ions and other buffer salts in the above Sigma products, each polynucleotide was dissolved in deionized water, 5 mg/mL, and dialyzed using Biotech CE dialysis tubing (MWCO 1000, Spectrum Laboratories, Inc.) against 5 mM LiBr aqueous solution for 24 h. The dialyzed solutions were then freeze-dried by vacuum.

Salmon sperm DNA (deoxyribonucleic acid sodium salt) is from Sigma and free of nitrate, thus is used without dialysis and other purification. The % G−C content is reported to be 41.2 [19] and the molecular weight is 1.3×10^6 (approximately 2000 bp).[20]

Glassy Samples. For polynucleotides 250 μL of MX aqueous (D_2O) solution containing 7 M LiBr was added directly to the freeze-dried dialyzed polynucleotides, forming 5 mg /mL solution. The ratios of base pairs (bp) to MX were determined by spectroscopic measurements with a Varian Cary UV−vis spectrophotometer. The base concentrations were determined by using the following molar extinction coefficients (M^{-1} cm^{-1}): polydAdT·polydAdT, 6600 at 260 nm;[18d] polydIdC·polydIdC, 6900 at 251 nm.[21] MX concentrations were determined by using the following molar extinction coefficients (M^{-1} cm^{-1}): 1.56×10^4 at 682 nm; 1.18×10^4 at 627 nm. The extinction coefficients for MX were derived from DNA−MX and assumed to be the same for polynucleotide−MX.

For DNA, 600 μL of deionized water (H_2O) was first added to 20 or 40 mg of DNA; then 1400 μL of MX aqueous (H_2O) solutions containing 10 M LiBr was added to dissolved DNA solutions. The ratios of bp to MX were determined by weight.

The resulting mixture was kept in the dark in a refrigerator for 7 days and stirred daily with a vortex mixer until the solution appeared homogeneous. Solutions were drawn into thin-wall 4 mm diameter Suprasil quartz tubes and then cooled to 77 K by immersing in liquid nitrogen resulting in glassy homogeneous samples. Upon adding MX solutions into solutions of polydAdT·polydAdT, polydIdC·polydIdC, and DNA, the blue color of MX became dark green, but in contrast, polydGdC·polydGdC−MX and polydG·polydC−MX remained as the original blue color. This result suggested that in 7 M LiBr MX was intercalated with DNA, polydAdT·polydAdT, and polydIdC·polydIdC, but not with polydGdC·polydGdC and polydG·polydC. This was confirmed by visible spectroscopy which showed no change in the MX spectrum in the presence of polydGdC·polydGdC and polydG·polydC and spectral shifts for MX with polydAdT·polydAdT, polydIdC·polydIdC, and DNA that indicate full binding with polynucleotides and DNA (see Figure 1).

The glassy samples were γ-irradiated for the absorbed dose of 0.7 kGy (20 min). On irradiation of the 7 M LiBr glass, the majority of initial ionization occurs in the solution and creates electrons and holes. The electrons are scavenged by the solutes and the holes remain in the glass as $Br_2•^-$. $Br_2•^-$ has a very broad ESR spectrum extending many hundreds of Gauss and does not interfere with the DNA and MX radical signals, which extend less than 75 G at 77 K.

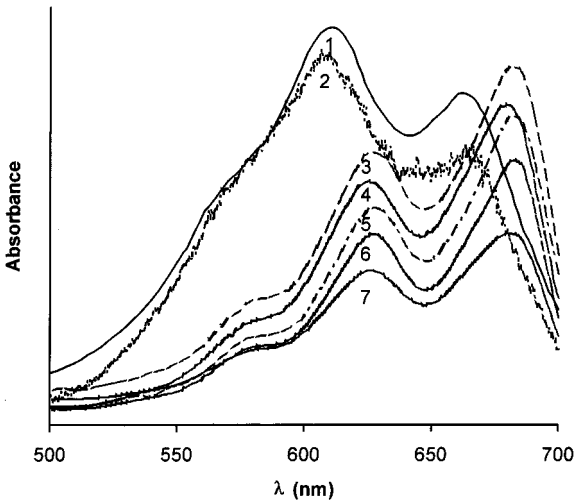

Figure 1. Visible spectra of MX and MX intercalated with polynucleotides and DNA. 1, MX in 7 M LiBr aqueous solution; 2, polydGdC·polydGdC and MX in 7 M LiBr (MX did not intercalate); 3, DNA−MX in 7 M LiBr; 4, polydAdT·polydAdT−MX in 7 M LiBr; 5, polydIdC·polydIdC−MX in 7 M LiBr; 6, polyA·polyU−MX in water; 7, polyC·polyG−MX in water. The visible spectra of MX and DNA−MX in water are not shown, but are the same as those in 7 M LiBr. The 20 nm red shift of MX in DNA, polydAdT·polydAdT, polydIdC·polydIdC, polyA·polyU, and polyC·polyG is expected for full intercalation of MX in DNA. In contrast, the spectrum of MX in polydGdC·polydGdC is the same as MX alone, and is in accord with unbound MX.

Frozen Samples. A 0.1 mL volume of MX aqueous (D_2O) solution was added to freeze-dried dialyzed polyA·polyU and polyC·polyG, forming 50 mg/mL polynucleotide. polyA·polyU−MX and polyCpolyG−MX gave visible spectra suggesting full intercalation of MX with polyA·polyU and polyC·polyG in D_2O, as shown in Figure 1. (We found that MX does not intercalate in pdC·pdG in 7 M LiBr even though it does in water solutions.) Frozen D_2O solutions (50 mg/mL) of polyA·polyU and polyC·polyG were prepared by adding 0.1 mL of D_2O to 10 mg of freeze-dried polyA·polyU and polyC·polyG, respectively. The resulting mixture was allowed to stand in the dark for several days with daily vortex mixing until the solid was dissolved homogeneously. The solution was drawn into a glass tube with inner diameter of 4 mm and frozen in liquid nitrogen; after warming the glass wall sufficiently the resultant ice plug was pushed out into liquid nitrogen. Like polynucleotide glassy samples, the ratios of bp to MX were determined by spectroscopic measurements with a Varian Cary UV−vis spectrophotometer. The base concentrations were determined by using the following molar extinction coefficients (M^{-1} cm^{-1}) at 260 nm: [18d] polyA·polyU, 7140; polyC·polyG, 8400. MX concentrations were determined by using the following molar extinction coefficients (M^{-1} cm^{-1}): 1.56×10^4 at 682 nm; 1.18×10^4 at 627 nm.

The ice samples were irradiated for 2.1 kGy (60 min). Frozen aqueous solutions of polynucleotide−MX consist of two phases: one is pure ice and the other is an amorphous region containing polynucleotide−MX and glassy water. Irradiation of the frozen aqueous solution produces both electrons and holes within polynucleotides as well as trapped •OH radicals in ice. Ice samples were annealed at 125 K for 3 min to remove the

ESR signal of ice phase •OH radicals before ESR analysis was performed.

All preparations were performed under nitrogen. Irradiated samples were kept in the dark in liquid nitrogen throughout all experiments. Deuterium oxide (D_2O) was from Aldrich with 99.9 atom % D. All polynucleotides were freezed-dried before sample preparation; after D_2O addition the deuteration was estimated to be around 98% complete.

Methods of Analysis. *Electron Spin Resonance*. ESR spectra were taken on a Varian Century Series EPR spectrometer operating at X-band with a dual cavity and a 200-mW klystron, with Fremy's salt ($g = 2.0056$, $A_N = 13.09$ G) as a reference. The spectra were recorded within a few minutes after irradiation, and at increasing time intervals thereafter.

Benchmark Spectra. Methods of analyses were similar to our previous work.[9−12] The benchmark spectra of MX radicals,[9] CD•, or T•− in 7 M LiBr (D_2O) glass[22] were used in the analysis of each experimental spectrum of appropriate glassy samples of polynucleotide−MX. The benchmark spectra of MX radicals and DNA base radicals in 7 M LiBr (H_2O) glass were obtained in this work and used in the analysis of each experimental spectrum of H_2O glassy samples of DNA−MX. The spectra in H_2O show greater ESR line widths than those in D_2O. The benchmark spectra of MX radicals in frozen DNA aqueous (D_2O) solution,[10] total base radicals in frozen polyA·polyU or polyC·polyG aqueous (D_2O) solution, were used in the analysis of each experimental spectrum of appropriate icy samples. Linear least-squares fitting of benchmark spectra to experimental spectra is employed to determine the fractional composition of base and MX radicals in each sample. The benchmark spectra of CD•,[22] T•−,[22] MX radicals, and DNA base radicals in 7 M LiBr (H_2O) glass, as well as total base radicals in frozen polyA·polyU or polyC·polyG aqueous (D_2O) solutions, are shown in Figure 2. MX radicals and DNA base radicals in 7 M LiBr (D_2O) glass are also included in Figure 2 for comparison.

Analysis for Transfer Distance and Tunneling Constants. For a random and complete intercalation, when the mole ratio of MX to polynucleotides or DNA base pairs (ν) is substantially less than 1, the probability that at least one MX is present within D_a base pairs from the trapped electrons or holes is well described by[9,13]

$$F(t) = 1 - (1 - \nu)^{2D_a(t)} \quad (1)$$

$F(t)$ also represents the fraction of all electrons and holes captured by MX at time t relative to all electrons and holes originally captured by the polynucleotide or DNA−MX system. The simple rearrangement of eq 1 leads to the relation for the time-dependent scavenging distance, $D_a(t)$:

$$D_a(t) = \frac{\ln(1 - F(t))}{2\ln(1 - \nu)} \quad (2)$$

For a tunneling process, the approximate relation for the time dependence of D_a, successfully used for tunneling kinetics in glasses[23] and in our previous work in DNA[9,10,12] is

$$D_a(t) = (1/\alpha)\ln(k_0 t) \quad (3)$$

where k_0 is the preexponential factor in the rate expression [$k = k_0 e^{-\beta D}$]; α is the apparent value of the distance decay constant β and is artificially reduced by interduplex electron transfer for DNA duplexes in close proximity as in the case of hydrated DNA samples or ices.[10] For frozen glassy solutions of a low concentration (5−20 mg/mL), the average center to center separations of the duplexes (150−300 Å) are far larger than electron transfer distances at our experimental condition; thus, the interduplex electron transfer is eliminated, α equals β, and D_a equals D_I, the transfer distance along the primary helix. For frozen water solutions of DNA (ices), the average center to center separation of the duplexes (23.1 Å)[24] is within electron transfer distances at our experimental condition and can be related to D_I via eq 4:[10]

$$D_a(t) = D_I(t) + n(D_I(t) - D_{ds}) \quad (4)$$

where $D_a(t)$, $D_I(t)$, and D_{ds} are in Å, n is the number of the adjacent DNA double strands, and D_{ds} is the interduplex center to center separation.

For polydAdT·polydAdT (average length 4219 bp), polydIdC·polydIdC (150−550 bp), and DNA (2000 bp) in glassy media, the average length for each polymer differs, but all are well above the electron/hole transfer distances found in this work (6−14 bp), and also are much greater than the ratio of bp to MX (17−51). Thus, we believe the lengths of the PNAs should not compromise our analytical assumptions. For icy samples, because polynucleotide strands are close together and inter double strand transfer makes a significant contribution to the

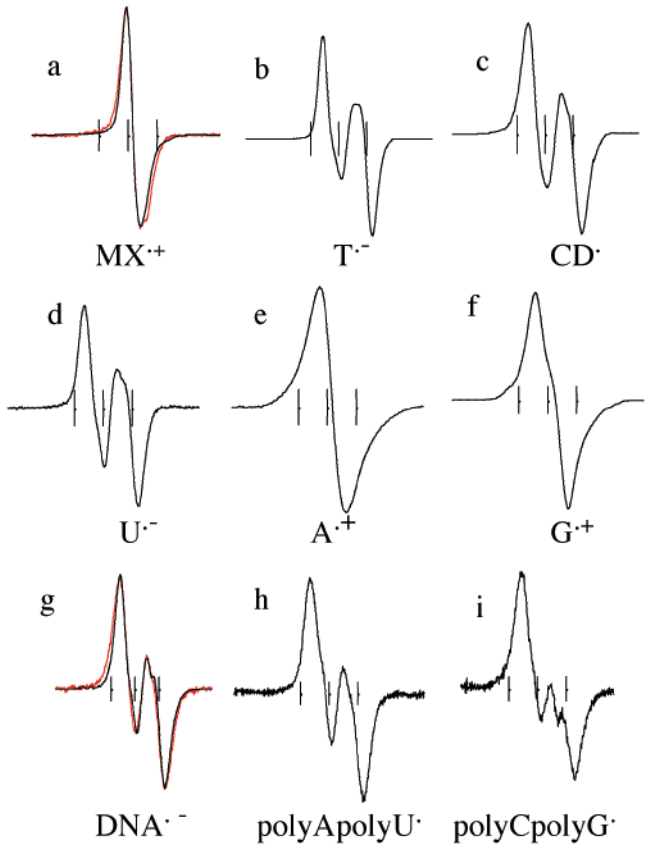

Figure 2. First derivative electron spin resonance "benchmark " spectra used in the analyses of polynucleotide−MX and DNA−MX complex systems. (a) One electron reduced $MX^{(2+)}$ ($MX•^{+}$) in frozen 7 M LiBr aqueous solution (black, D_2O; red, H_2O). Deoxyribonucleotide radicals: (b) $T•^{-}$, (c) CD•, and (d) $U•^{-}$ in frozen 7 M LiBr aqueous (D_2O) solution; (e) $A•^{+}$ and (f) $G•^{+}$ in frozen 8 M $NaClO_4$ aqueous (D_2O) solutions. (g) DNA anion radical in frozen 7 M LiBr aqueous solution (black, D_2O; red, H_2O). (h) One electron reduced and oxidized species in polyA·polyU and (i) polyC·polyG in irradiated frozen D_2O solutions. The three markers are each separated by 13.09 G. The central marker is at $g = 2.0056$. Other base functions of similar shape for $T•^{-}$, CD•, and $U•^{-}$ from polynucleotides in ices were also employed for ice samples.

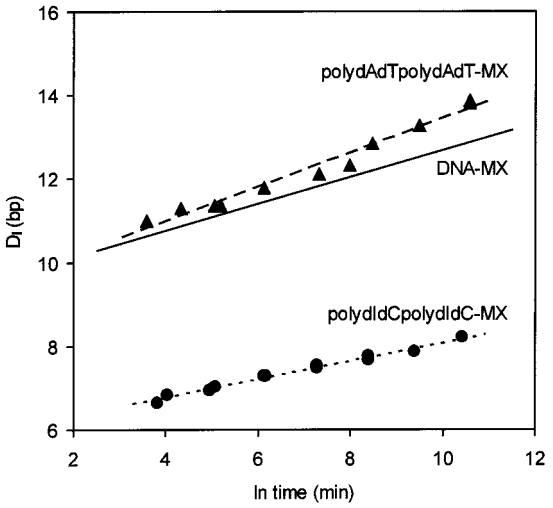

Figure 3. Plot of electron transfer distance D_I vs natural logarithm of time in minutes after irradiation for polydAdT·polydAdT−MX (bp/MX = 17, 5 mg polynucleotide/mL) and polydIdC·polydIdC−MX (bp/MX = 36, 5 mg polynucleotide /mL) in frozen glassy 7 M LiBr aqueous (D_2O) solutions at 77 K. The transfer distance is calculated from the fraction of MX radicals in the overall ESR spectrum using eq 2. Lines are fit to eq 3. As a comparison, a plot of D_I vs natural log of time for DNA−MX in frozen glassy 7 M LiBr aqueous (D_2O) solutions at 77 K, with $\beta = 0.92$ Å^{-1} and $D_I(1') = 9.5$ bp, is also included.[9,10]

observed overall transfer distance, even the low ratios of MX to bp used (1/100) should not significantly challenge our analytical assumptions.

Results

Glassy Samples. *Polynucleotides.* The ESR signals of irradiated samples of polydAdT·polydAdT−MX (molar ratio of MX to bp, ν, 1/17), polydIdC·polydIdC−MX (ν 1/36), polydGdC·polydGdC−MX(ν 1/20), and polydG·polydC−MX-(ν 1/20) in 7 M LiBr at 77 K were followed at increasing time intervals after irradiation. The polynucleotide concentration was about 5 mg/mL. Linear least-squares fits of benchmark spectra to experimental spectra yield estimates of the fractions of MX radical (MX•$^+$) and one electron reduced cytosine (CD•) for polydIdC·polydIdC−MX, polydGdC·polydGdC−MX, and polydG·polydC−MX relative to the total radicals formed in polynucleotides. For polydAdT·polydAdT−MX the fits yield the fractions of MX radical (MX•$^+$) and thymine anion radical (T•$^-$). The fraction of MX•$^+$ increased with time for polydAdT·polydAdT−MX, polydIdC·polydIdC−MX; however, no change was noted for polydGdC·polydGdC−MX and polydG·polydC−MX. Visible spectroscopy (Figure 1) showed that MX was not intercalated in these latter two polynucleotides in 7 M LiBr. These "failed" experiments acted as controls showing that transfer was only along the DNA strand in dilute solutions of the polynucleotides. The distances of electron transfer along polynucleotide double strands are derived from eq 2. Plots of the ET distance (D_I) vs natural log of time are given in Figure 3 for polydAdT·polydAdT−MX, polydIdC·polydIdC−MX. As a comparison, a plot of D_I vs natural log of time for DNA−MX with $\beta = 0.92 \pm 0.1$ Å^{-1} and $D_I(1') = 9.5 \pm 1$ bp is also included in Figure 3.[9,10] The linearity in ET distance with natural log of time is in accord with a single step tunneling process. The linear least-squares fits of eq 3 to the data gave the following values of electron tunneling constant β and ET distances at 1 min: 0.75 ± 0.1 Å^{-1} and 9.4 ± 0.5 bp for polydAdT·polydAdT, 1.4 ± 0.1 Å^{-1} and 5.9 ± 0.5 bp for polydIdC·polydIdC, respectively.

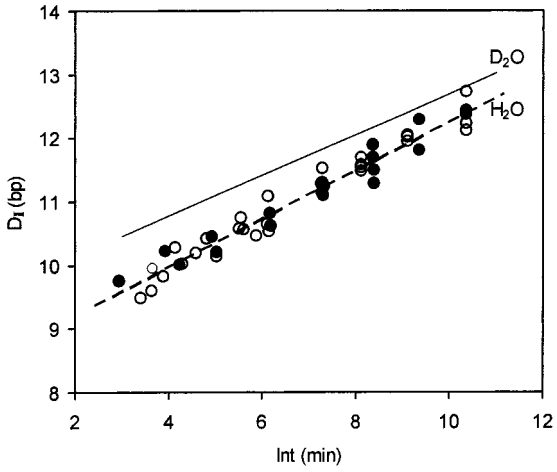

Figure 4. Plot of electron transfer distance D_I vs natural logarithm of time in minutes after irradiation for DNA−MX (bp/MX = 51, filled circles, 10 mg/mL; open circles, 20 mg/mL) in frozen glassy 7 M LiBr aqueous (H_2O) solutions at 77 K. The transfer distance is calculated from the fraction of MX radicals in the overall ESR spectrum using eq 2. Lines are fit to eq 3. As a comparison, a plot of D_I vs natural log of time for DNA−MX in frozen glassy 7 M LiBr aqueous (D_2O) solutions at 77 K, with $\beta = 0.92$ Å^{-1} and $D_I(1') = 9.5$ bp, is also included.[9,10] The slightly smaller intercept and larger slope for H_2O than D_2O suggest only a modest D/H isotope effect.

Isotope Effect. The ESR signals of irradiated samples of DNA−MX (molar ratio of MX to bp, ν, 1/51, DNA concentration: 10 or 20 mg/mL) in 7 M LiBr (H_2O) at 77 K were followed at increasing time intervals after irradiation. Linear least-squares fits of benchmark spectra to experimental spectra yield estimates of the fractions of MX radical (MX•$^+$) and DNA base radicals (CH$^\bullet$ + T•$^-$). The fraction of MX•$^+$ increased with time as expected for ET from the reduced species (CH$^\bullet$ + T•$^-$) to MX. The distances of electron transfer along DNA double strands are derived from eq 2. Plots of the ET distance (D_I) vs natural log of time are given in Figure 4. A plot of D_I vs natural log of time for DNA−MX in 7 M LiBr (D_2O) is also included in Figure 4 for comparison, with $\beta = 0.92 \pm 0.1$ Å^{-1} and $D_I(1') = 9.5 \pm 1$ bp.[9,10] The linear least-squares fits of eq 3 to the data gave 0.8 ± 0.1 Å^{-1} for the value of electron tunneling constant β and an ET distances at 1 min of 8.5 ± 1.0 bp for DNA−MX in 7 M LiBr (H_2O) at 77 K. The slightly smaller β and $D_I(1')$ over those found in D_2O suggests a modest isotope effect on excess electron transfer along DNA double strands at 77 K.

Frozen Polynucleotide D_2O Solutions (Icy Samples). The ESR signals of samples of polyA·polyU−MX and polyC·polyG−MX (molar ratio of MX to bp as 1/100, polynucleotide concentration: 50 mg/mL) in frozen aqueous (D_2O) solutions at 77 K were followed at increasing time intervals after irradiation. Linear least-squares fits of benchmark spectra to experimental spectra yield estimates of the fraction of total radicals which are MX radicals (MX•$^+$) and base radicals (A•$^+$ + U$^{\bullet-}$for polyA·polyU and G•$^+$ + CD$^\bullet$ for polyC·polyG, respectively.). Figure 5 shows first derivative electron spin resonance spectra found 400 min after γ-irradiation of the above polyA·polyU−MX and polyC·polyG−MX at 77 K. The linear least-squares fits of benchmark spectra to each experimental spectrum are also shown for comparison. The spectra and analyses show that the fraction of MX radicals in polyA·polyU−MX (70%) is twice that in polyC·polyG−MX (40%). The fraction of MX•$^+$ increased with time for both samples. The apparent distances of electron and hole transfer along polynucleotide double strands are derived from eq 2. Plots of the

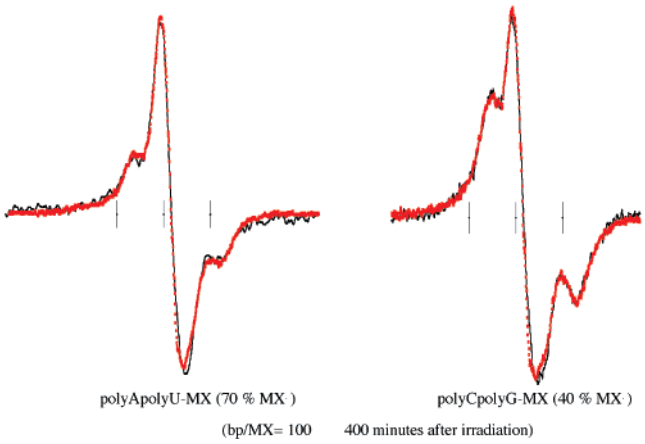

Figure 5. First derivative electron spin resonance spectra found 400 min after γ-irradiation of polyA·polyU−MX and polyC·polyG−MX in frozen aqueous (D_2O) solutions at 77 K. The ratio of bp to MX is 100/1 and the concentration is 50 mg/mL for both samples. The spectra clearly show that the fraction of MX radicals in the spectrum of polyA·polyU−MX is far larger than that in polyC·polyG−MX. The red lines are the linear least-squares fits of benchmark ESR spectra to experimental spectra (black). The three markers are each separated by 13.09 G. The central marker is at $g = 2.0056$.

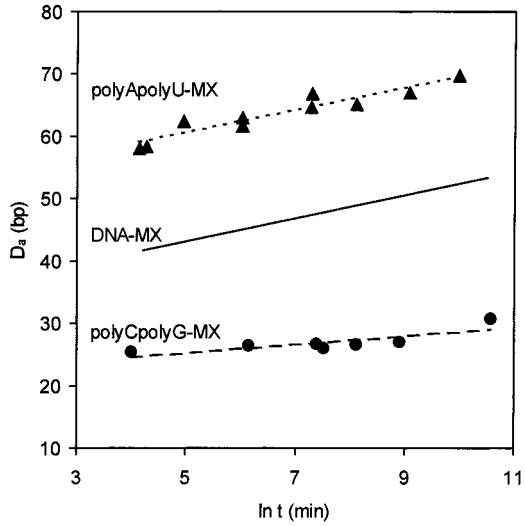

Figure 6. Plot of apparent electron- and hole-transfer distance (D_a-(MX•)) vs natural logarithm of time in minutes after irradiation for polyA·polyU−MX and polyC·polyG−MX in frozen aqueous solutions (D_2O ices) at 77 K. The transfer distance is calculated from the fraction of MX radicals in the overall ESR spectrum using eq 2. Lines are fit to eq 3. As a comparison, a plot of D_a vs natural log of time for DNA−MX in frozen aqueous (D_2O) solutions at 77 K, with $\alpha = 0.16$ Å^{-1} and $D_a(1') = 34$ bp, is also included.[10] The transfer distances appear far larger in frozen ices than in glassy solutions because DNA strands in the ices are in close proximity, allowing for interduplex transfer. Accounting for this brings the transfer distance along one strand into close agreement with that found in glasses where the solutions are homogeneous.

apparent ET distance in polyApolyU−MX and polyC·polyG−MX vs natural log of time are given in Figure 6. As a comparison, a plot of D_a vs natural log of time for DNA−MX in frozen D_2O aqueous solution with $\alpha = 0.16 \pm 0.04$ Å^{-1} and $D_a(1') = 34 \pm 3$ bp is also included in Figure 6.[10] The linearity in ET distance with log time again implies a single step tunneling process. The linear least-squares fits of eq 3 to the data gave the values of apparent electron tunneling constant α and ET distances at 1 min: 0.2 ± 0.1 Å^{-1} and 52 ± 5 bp for polyA·polyU as well as 0.4 ± 0.1 Å^{-1} and 22 ± 5 bp for polyC·polyG, respectively. The distances are increased and the distance decay constants are reduced by interduplex transfer.

Discussion

The effect of base sequence on electron transfer in polynucleotides and DNA is apparent from our results. Figure 3 suggests a somewhat faster electron transfer in polydAdT·polydAdT−MX than in DNA at 77 K, whereas the transfer in polydIdC·polydIdC−MX was far slower. Our recent DFT theoretical study[14] and the experimental study of Steenken et al.[15] show that GC[14,15] and IC[14] anion radicals are "unstable" in their initial structures and proton transfer is energetically favorable for both. The predicted free energy change for the proton transfer for GC anion radical is −3 kcal/mol with small activation energy of 1 kcal/mol. Remarkably, theory suggests the I−C anion radical system shows no significant activation energy toward proton transfer and a large free energy change favoring the proton transferred state (−7 kcal).[14] Thus, the proton transfer from I to C•$^-$ should follow immediately after the anion radical is formed, whereas the transfer from G to C•$^-$ owing to its activation barrier might be slightly slower than from I to C•$^-$. For the AT base pair, experiment and theory agree that proton transfer from A to T•$^-$ does not occur.[15,16] Thus, the significant difference of ET between polydAdT·polydAdT−MX and polydIdC·polydIdC−MX suggests that the proton transfer between I and C•$^-$ forming CH• substantially hinders electron transfer. We find that electron transfer in polydAdT·polydAdT is only slightly faster than in DNA at 77 K. Since in DNA the electron adduct of C is a significant fraction of the DNA electron adducts, the comparable rate in polydAdT·polydAdT suggests a lesser effect of protonation on the energetics of transfer from GC than from IC. We attribute this to the fact that the proton transfer from G to C•$^-$ is less favorable than that from I to C•$^-$. This combined with the substantial amounts of T•$^-$ due to the initial slightly higher electron affinity of T than C [25] results in the electron transfer rate in DNA being closer to that of polydAdT·polydAdT than polydIdC·polydIdC.

While a large and growing number of studies address electron and hole transfer in DNA, only a few involve polynucleotides with inosine. Wan et al.[3] found the charge transfer from Ap* (the lowest excited state of 2-aminopurine) to I was energetically unfavorable in both directions of oxidation and reduction; thus they used I as a calibration base for quantifying the G oxidation rates. Kelley et al.[26] used I as C's complementary bases in order to incorporate only one single GC base step in their self-assembled monolayer of DNA film and constrain the intercalator, daunomycin, in the GC step. Inosine was not found to have any effect in electron transfer in DNA films; however, the electron transfer through the 10 Å σ-bonded linker was likely the rate-determining step, which would mask any effect of base sequence. In our study, polydIdC·polydIdC played a different role. In 7 M LiBr MX is fully intercalated within polydIdC·polydIdC but does not significantly intercalate in polydGdC·polydGdC or polydG·polydC in LiBr. Thus, polydIdC·polydIdC acted as an alternative polynucleotide for us to study the effect of proton transfer between base pairs on excess electron transfer. However, polydIdC·polydIdC and polydGdC·polydGdC are not truly equivalent, since "I" has both a higher electron affinity and higher ionization potential than G.

While we believe the values of $D_l(1')$ in D_2O and H_2O are within experimental error, the smaller values of β for the electron transfer in DNA in H_2O over D_2O media may be significant. This can be explained by the greater stability of CD• over CH•

TABLE 1: Transfer Distances and Distance Decay Constants for Electron and Hole Transfer to MX in Polynucleotides−MX and DNA−MX at 77 K

polynucleotide	medium	transferring species	$D_I(1')$ (bp)	decay const[d] ($Å^{-1}$)
polydAdT·polydAdT	D_2O glass[a]	$T^{\bullet-}$	9.4 ± 0.5	$\beta = 0.75 \pm 0.1$
polydIdC·polydIdC	D_2O glass	$CD^{\bullet}$	5.9 ± 0.5	$\beta = 1.4 \pm 0.1$
DNA	H_2O glass	$T^{\bullet-} + CH^{\bullet}$	8.5 ± 1.0	$\beta = 0.8 \pm 0.1$
DNA[9]	D_2O glass	$T^{\bullet-} + CD^{\bullet}$	9.5 ± 0.5	$\beta = 0.92 \pm 0.1$
polyA·polyU	D_2O ice[b]	$A^{\bullet+} + U^{\bullet-}$	$52 \pm 5/13$[c]	$\alpha = 0.2 \pm 0.1$
		$A^{\bullet+}$	$48 \pm 10/13$[c]	
		$U^{\bullet-}$	$60 \pm 10/14$[c]	
polyC·polyG	D_2O ice	$G^{\bullet+} + CD^{\bullet}$	$22 \pm 5/9$[c]	$\alpha = 0.4 \pm 0.1$
		$G^{\bullet+}$	$15 \pm 5/8$[c]	
		$CD^{\bullet}$	$38 \pm 5/11$[c]	
DNA[10,12]	D_2O ice	$G^{\bullet+} + CD^{\bullet} + T^{\bullet-}$	$34 \pm 3/10.7$[c]	$\alpha = 0.16 \pm 0.04$
		$G^{\bullet+}$	$17 \pm 5/8$[c]	
		$CD^{\bullet} + T^{\bullet-}$	$42 \pm 5/12$[c]	

[a] Glass indicates frozen 7 M LiBr aqueous solutions. [b] Ice refers to frozen aqueous solutions which form an crystalline ice phase and pockets of solid and hydration waters. [c] The first value is $D_a(1')$ and the second is $D_I(1')$ which is estimated by eq 4,[10] taking n as 6 and D_{ds} as 23.1 Å.[24] [d] β is the usual distance decay constant for a single DNA duplex whereas α uses the same relationship but is substantially reduced in magnitude by duplex to duplex transfer. The distances between duplexes greatly affect the value of α.

(the zero point energy of $CD^{\bullet}$ will be ca. 1 kcal lower in energy than CH•). This provides slightly weaker driving force for electron transfer from CD• to MX than from CH•; thus, the value of β is expected to be larger in D_2O than in H_2O. D_2O likely also slows protonation and thus might extend the initial time period of fast electron transfer from $C\bullet^-$ (raising $D_I(1')$); however, after protonation (or deuteration) D_2O creates a more stable state for the C electron adduct as CD• which slows subsequent electron transfer and raises β. Since these provocative results are at the fringe of significance, more work will be necessary before any firm conclusions can be made.

Recently Shafirovich et al. reported a kinetic deuterium isotope effect on proton-coupled electron transfer reactions at a distance in DNA duplexes.[17b] In their study, the electron donor is G and the electron acceptor is a neutral radical, 2AP(−H)•. In their experiments, faster deprotonation and protonation of the products in H_2O than in D_2O provide stronger driving force for the hole transfer. In contrast, in our experiment, the electron donor (the reactant) is protonated prior to the electron transfer, and the fact that CD• has greater stability than CH• results in a slower transfer and larger β in D_2O than in H_2O.

As with polynucleotides in glassy samples, the effect of base sequence on electron and hole transfer in frozen water solutions of DNA and polyribonucleotides (icy samples) can also be found from our results. Figure 6 shows a farther electron and hole transfer distance in polyA·polyU than in DNA at 77 K in the time scale of days to weeks, whereas the transfer distance in polyC·polyG was far shorter. The situation for icy samples is more complicated than that for glassy samples, since in glassy samples only electron transfer along double strands is involved but in icy samples both hole and electron transfers contribute; in addition, inter double strand transfer also contributes significantly in icy samples. Although these results could be complicated by recombination of holes and electrons within the DNA and at the MX acceptor, our previous work showed this effect is small at loadings employed in this work.[12] Thus, as expected, ESR signal intensities for both icy polyA·polyU and polyC·polyG remain constant within experimental error through the time course of measurement. U has an electron affinity similar to that of T[25] and thus polyA·polyU acts as a comparison model for polydAdT·polydAdT. As in the case of AT base pairs, proton transfer in AU base pair ion radicals is not expected. However, full proton transfer is expected in $GC\bullet^-$ and partial transfer is expected in $GC\bullet^+$. Proton transfer in $GC\bullet^-$ and $GC\bullet^+$ slows electron and hole transfer and thus provides an explanation for the decreasing order of *overall* electron and hole transfer distances shown in Figure 6: polyA·polyU > DNA > polyC·polyG. Note the values for D_a in the figure do not represent the distance for electron transfer along one duplex, which is far smaller (see Table 1).

Assuming the packing of the strands in frozen solutions of polyA·polyU, polyC·polyG is similar to DNA in frozen ices, the transfer distance along the primary helix can be estimated by eq 4[10] from the overall apparent transfer distances D_a of 52 bp for polyA·polyU, 34 bp for DNA, and 22 bp for polyC·polyG. Take n as 6 (for hexagonal packing) and $D_{ds} = 23.1$ Å.[24] The average hole and electron transfer distance along the primary helix ($D_I(1')$) in frozen ice decreases in the following order: polyA·polyU (13 bp) > DNA (11 bp) > polyC·polyG (9 bp). These results would be expected from the prototropic equilibria within the base pairs, which do not affect AT or AU base pairs but occur in GC base pairs in polyC·polyG and DNA.

The fractions of $A\bullet^+$ and $U\bullet^-$ in polyA·polyU−MX, relative to total radicals formed in polyA·polyU, were estimated by linear least-squares fits of benchmark spectra of $MX\bullet^+$, $A^{\bullet+}$,[22] and $U^{\bullet-}$ [22] to experimental spectra. The fraction of $A\bullet^+$ and $U\bullet^-$ in polyA·polyU (without MX) were also obtained by linear least-squares fits. With methods described previously,[12] D_a and D_I at the time scale of our experiment were found to be 48 ± 10 bp and ca. 13 bp for $A\bullet^+$ and 60 ± 10 bp and ca. 14 bp for $U\bullet^-$, respectively. Similarly, based on the fractions of $G\bullet^+$ and CD• in polyC·polyG−MX as well as polyC·polyG, D_a and D_I were estimated to be 15 ± 5 bp and ca. 8 bp for $G\bullet^+$ and 38 ± 5 bp and ca. 11 bp for CD•, respectively. Though the analytical errors for the above values of D_a and D_I are relatively high, it is obvious that $A\bullet^+$ transfers much farther than $G\bullet^+$ and $U\bullet^-$ farther than CD•. We attribute these to both the effect of interbase pair proton transfer in both GC anion and cation radicals, and the higher driving force for transfer for $A\bullet^+$ over that for $G\bullet^+$. The fact that the total transfer distances, $D_a(1')$, for $G\bullet^+$ found from polyC·polyG (15 ± 5 bp) and DNA (17 ± 5 bp)[12] are in good agreement suggests at low temperatures there is no great benefit to a homopolymer stack of G's over the DNA "assortment" of sequences.

Giese et al.[2] found at room temperature that hole transfer from $G\bullet^+$ to GGG involves both single-step tunneling and thermally induced "G" or "A" hopping processes; which mechanism plays the main role depends on the sequence. At the low temperature of 77 K, hopping is not activated, and as a consequence in our experiments only tunneling is observed. Interestingly, we find tunneling from $A\bullet^+$ to MX extends to far greater distances than that found for $G^{\bullet+}$ to MX.

This work studies the excess electron transfer in polydAdT·polydAdT, polydIdC·polydIdC, polyC·polyG, polyA·polyU, and salmon sperm DNA. The base sequences are known for the former four polymers, but not for DNA. For DNA, only the content percent of AT vs GC is known. These commercially available PNAs provide us a fruitful approach to gain initial insights on the effect of base sequence on electron transfer in DNA. With these sequences we are unable to determine the more detailed effect of base sequences. Therefore, studies on ET in various known sequences of polynucleotides at different lengths are essential in further work.

The transfer distances at 1 min after irradiation found in this work are compiled in Table 1. For comparison, the previously reported data for DNA−MX in both frozen 7 M LiBr aqueous (D_2O) solutions and frozen aqueous (D_2O) solutions are also shown in Table 1.

Conclusions

Our major findings are the following.

1. Electron transfer in DNA is clearly base sequence dependent. We find that excess electron transfer through polydAdT·polydAdT extends to substantially longer distances than through polydIdC·polydIdC at 77 K. We attribute this in part to proton transfer from I to C•$^-$ forming CH•, which substantially slows the transfer rates in polydIdC·polydIdC. Intra base pair proton transfer processes are not likely in polydAdT·polydAdT.[15,16]

2. Excess electron transfer through salmon testes DNA is intermediate between polydAdT·polydAdT and polydIdC·polydIdC. In DNA about equal amounts of T and C electron adducts are present at 77 K[27] and transfer from both is expected. Thus the rate of transfer found in DNA is a blend of these two rates. Proton transfer from G to C•$^-$ forming CH• should slow electron transfer so that the transfer from C electron adducts is substantially less than that from T•$^-$. Thus it makes sense that DNA should be intermediate between the two polydeoxynucleotides, polydAdT·polydAdT and polydIdC·polydIdC. The fact that DNA is much closer to polydAdT·polydAdT than polydIdC·polydIdC suggests that electron transfer from a GC base pair in DNA is not as slow as from an IC base pair in polydIdC·polydIdC. This result is in agreement with theoretical calculations of the thermodynamic driving force for proton transfer within the GC and IC base pair radical anions that show the IC base proton transfer is far more exergonic.[14]

3. Excess electron and hole transfer in salmon testes DNA is also intermediate between polyA·polyU and polyC·polyG. This result again suggests that both proton transfer from G to C•$^-$ forming CH• and the partial transfer from G•$^+$ to C forming G(−H)• slow the transfer rates in DNA and polyC·polyG. Like polydAdT·polydAdT, proton transfer processes are not thought to be present in polyA·polyU. As expected from these processes, the hole transfer from A•$^+$ to MX is found to be faster than that from G•$^+$, whereas the electron transfer from U•$^-$ to MX is faster than that from CD•.

4. In our previous work on electron transfer in DNA we noted that the ESR signal from T•$^-$ appeared to diminish while that of one-electron-reduced C was nearly unchanged in time.[11,12] From this we concluded that either the electron transfer in DNA to MX was from T•$^-$ solely or that transfer from one-electron-reduced C to MX was compensated by a transfer from T•$^-$ to C creating a constant steady-state concentration of one-electron-reduced C. In our recent work[12] supplemental information was presented that in DNA alone (no intercalator) transfer occurs over time from T•$^-$ to C. In the present work we observe a modest D/H isotope effect in excess electron transfer through DNA which also is in accord with electron transfer in DNA from both T and C electron adducts. In addition, our results for polyC·polyG, polydIdC·polydIdC in this work also convincingly show that electron transfer from CH• to the MX acceptor occurs but at a slower rate than from T•$^-$. As previously stated, we attribute this to the proton transfer in the GC base pair anion. We note, however, that theoretical work[16] confirmed by higher level work in progress suggests that the GC anion radical has a slightly higher electron affinity than the AT anion radical predicting the inherent electron transfer from GC anion radical to be slower. Proton transfer then further slows the transfer rate.

Acknowledgment. This research was supported by NIH NCI Grant RO1CA45424 and by the Oakland University Research Excellence Fund.

References and Notes

(1) (a) Lewis, F. D.; Liu, X.; Liu, J.; Miller, S. E.; Hayes, R. T.; Wasielewski, M. R. *NATURE (London)* **2000**, *406*, 51−3. (b) Lewis, F. D.; Kalgutkar, R. S.; Wu, Y.; Liu, X.; Liu, J.; Hayes, R. T.; Miller, S. E.; Wasielewski, M. R. *J. Am. Chem. Soc.* **2000**, *122*, 12346−51. (c) Lewis, F. D.; Liu, X.; Liu, J.; Hayes, R. T.; Wasielewski, M. R. *J. Am. Chem. Soc.* **2000**, *122*, 12037−8. (d) Lewis, F. D.; Zhang, Y.; Liu, X.; Xu, N.; Letsinger, R. L. *J. Phys. Chem.* **1999**, *103*, 2570−2578. (e) Lewis, F. D.; Wu, T.; Zhang, Y.; Letsinger, R. L.; Greenfield, S. R. *Science* **1997**, *277*, 673−6.

(2) (a) Giese, B.; Amaudrut, J.; Kohler, A.; Sportmann, M. a. W. S. *Nature* **2001**, *412*, 318−320. (b) Giese, B. *Acc. Chem. Res.* **2000**, *33*, 631−6. (c) Giese, B.; Wessely, S.; Spormann, M.; Ute Lindemann, S.; Meggers, E.; Michel-Beyerle, M. E. *Angew. Chem., Int. Ed.* **1999**, *38*, 996−998. (d) Meggers, E.; Dussy, A.; Schäfer, T.; Giese, B. *Chemistry* **2000**, *6*, 485−92.

(3) (a) Wan, C.; Fiebig, T.; Schiemann, O.; Barton, J. K.; Zewail, A. H. *Proc. Natl. Acad. Sci. U.S.A.* **2000**, *97*, 14052−5. (b)Wan, C.; Kelley, S. O.; Barton, J. K.; Zewail, A. H. *Proc. Natl. Acad. Sci. U.S.A.* **1999**, *96*, 1187−92.(c)Wan, C.; Fiebig, T.; Kelley, S. O.; Treadway, C. R.; Barton, J. K.; Zewail, A. H. *Proc. Natl. Acad. Sci. U.S.A.* **1999**, *96*, 6014−9.

(4) (a) Núñez, M. E.; Barton, J. K. *Curr. Opin. Chem. Biol.* **2000**, *4*, 199−206. (b) Núñez, M. E.; Rajski, S. R.; Barton, J. K. *Methods Enzymol.* **2000**, *319*, 165−88. (c) Kelley, S. O.; Barton, J. K. *Science* **1999**, *283*, 375−81.

(5) (a) Berlin, Y. A.; Burin, A. L.; Ratner, M. A. *J. Am. Chem. Soc.* **2001**, *123*, 260−8. (b) Berlin, Y. A.; Burin, A. L.; Siebbeles, L. D. A.; Ratner, M. A. *J. Phys. Chem. A* **2001**, *105*, 5666−5678. (c) Grozema, F. C.; Berlin, Y. A.; Siebbeles, L. D. A. *Int. J. Quantum Chem.* **1999**, *75*, 1009−16. (d) Grozema, F. C.; Berlin, Y. A.; Siebbeles, L. D. A. *J. Am. Chem. Soc.* **2000**, *122*, 10903−9. (e) Berlin, Y. A.; Burin, A. L.; Ratner, M. A. *J. Phys. Chem. A* **2000**, *104*, 443−5.

(6) (a) Bixon, M.; Jortner, J. *J. Phys. Chem. B* **2000**, *104*, 3906−3913. (b) Jortner, J.; Bixon, M.; Langenbacher, T.; Michel-Beyerle M. E. *Proc. Natl. Acad. Sci. U.S.A.* **1998**, *95*, 12759−65. (c) Bixon, M.; Giese, B.; Wessely, S.; Langenbacher, T.; Michel-Beyerle, M. E.; Jortner, J. *Proc. Natl. Acad. Sci. U.S.A.* **1999**, *96*, 11713−6. (d) Voityuk, A. A.; Jortner, J.; Bixon, M.; Rösch, N. *Chem. Phys. Lett.* **2000**, *324*, 430−4. (e) Nitzan, A.; Jortner, J.; Wilkie, J.; Burin, A. L.; Ratner, M. A. *J. Phys. Chem. B* **2000**, *104*, 5661−5665. (f) Voityuk, A. A.; Rösch, N.; Bixon, M.; Jortner, J. *J. Phys. Chem. B* **2000**, *104*, 9740−9745.

(7) (a) Debije, M. G.; Strickler, M. D.; Bernhard, W. A. *Radiat. Res.* **2000**, *154*, 163−170. (b) Debije, M. G.; Bernhard, W. A. *J. Phys. Chem. B* **2000**, *104*, 7845−51. (c) Debije, M. G.; Bernhard, W. A. *Radiat. Res.* **1999**, *152*, 583−9. (d) Milano, M. T.; Bernhard, W. A. *Radiat. Res.* **1999**, *152*, 196−201. (e) Debije, M. G.; Milano, M. T.; Bernhard, W. A. *Angew. Chem., Int. Ed.* **1999**, *38*, 2752−6. (f) Bernhard, W. A.; Milano, M. T. *Radiat. Res.* **1999**, *151*, 39−49.

(8) Razskazovskii, Y.; Swarts, S. G.; Falcone, J. M.; Taylor, C.; Sevilla, M. D. *J. Phys. Chem. B* **1997**, *101*, 1460−7.

(9) Messer, A.; Carpenter, K.; Forzley, K.; Buchanan, J.; Yang, S.; Razskazovkii, Y.; Cai, Z.; Sevilla, M. D. *J. Phys. Chem. B* **2000**, *104*, 1128−36.

(10) Cai, Z.; Sevilla, M. D. *J. Phys. Chem. B* **2000**, *104*. 6942−9.

(11) Cai, Z.; Gu, Z.; Sevilla, M. D. *J. Phys. Chem. B* **2000**, *104*, 10406−10411.

(12) Cai, Z.; Gu, Z.; Sevilla, M. D. *J. Phys. Chem. B* **2001**, *105*, 6031−6041.

(13) Anderson, R. F.; Wright, G. A. *Phys. Chem. Chem. Phys.* **1999**, *1*, 4827−31.

(14) Li, X.; Cai, Z.; Sevilla, M. D. *J. Phys. Chem. B* **2001**, *105*, 10115−23.

(15) (a) Steenken, S. *Biol. Chem.* **1997**, *378*, 1293−7. (b) Steenken, S. *Chem. Rev.* **1989**, *89*, 503.

(16) (a) Colson, A. O.; Besler, B.; Close, D. M.; Sevilla, M. D. *J. Phys. Chem.* **1992**, *96*, 661−668. (b) Colson, A. O.; Besler, B.; Sevilla, M. D. *J. Phys. Chem.* **1992**, *96*, 9788−9794. (d) Colson, A. O.; Sevilla, M. D. *Int. J. Radiat. Biol*. **1995**, *67*, 627−645. (e) Colson, A. O.; Sevilla, M. D. *J. Phys. Chem*. **1995**, *99*, 3866−3874. (f) Colson, A. O.; Sevilla, M. D. *J. Phys. Chem.* **1995**, *99*, 13033−13037. (g) Sevilla, M. D.; Besler, B.; Colson, A. O. *J. Phys. Chem*. **1995**, *99*, 1060−1063.

(17) (a) Weatherly, S. C.; Yang, I. V.; Thorp, H. H. *J. Am. Chem. Soc.* **2001**, *123*, 1236−7. (b) Shafirovich, V.; Dourandin, A.; Geacintov, N. E. *J. Phys. Chem. B* **2001**, *105*, 8431−5.

(18) (a) Kelley, S. O.; Barton, J. K. *Chem. Biol.* **1998**, *5*, 413−25. (b) Stemp, E. D.; Barton, J. K. *Inorg. Chem.* **2000**, *39*, 3868−3874. (c) Núñez, M. E.; Hall, D. B.; Barton, J. K. *Chem. Biol.* **1999**, *6*, 85−97. (d) Barton, J. K.; Goldberg, J. M.; Kumar, C. V.; Turro, N. J. *J. Am. Chem. Soc.* **1986**, *108*, 2081−8.

(19) Marmur, J.; Doty, P. *J. Mol. Biol.* **1962**, *5*, 109−118.

(20) Tanaka, K.; Okahata, Y. A. *J. Am. Chem. Soc*. **1996**, *118*, 10679−83.

(21) Baguley, B. C.; Falkenhaug, E. M. *Nucleic Acids Res.* **1978**, *5*, 161.

(22) Yan, M.; Becker, D.; Summerfield, S.; Renke, P.; Sevilla, M. D. *J. Phys. Chem.* **1992**, *96*, 1983−9.

(23) Khairutdinov, R. F.; Zamaraev, K. I. *Russ. Chem. Rev.* **1978**, *47*, 518−530.

(24) Lee, S. A.; Lindsay, M.; Powell, J. W.; Weidlich, T.; Tao, N. J.; Lewen, G. D. *Biopolymers* **1987**, *26*, 1637−66.

(25) Li, X.; Cai, Z.; Sevilla, M. D. *J. Phys. Chem. A* **2002**, *106*, 1596.

(26) Kelley, S. O.; Jackson, N. M.; Hill, M. G.; Barton, J. K. *Angew. Chem., Int. Ed.* **1999**, *38*, 941−5.

(27) Wang, W.; Yan, M.; Becker, D.; Sevilla, M. D. *Radiat. Res.* **1994**, *137*, 2−10.